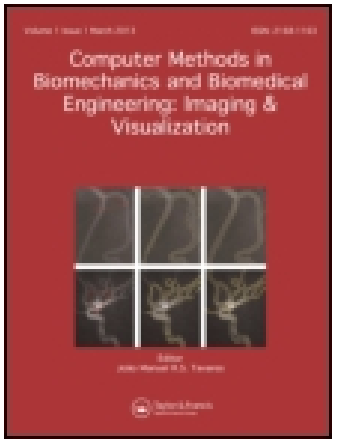

Computer Methods in Biomechanics and Biomedical Engineering: Imaging & Visualization
Publication details, including instructions for authors and subscription information:
http://www.tandfonline.com/loi/tciv20

Reduced lead system selection methodology for reliable standard 12-lead reconstruction targeting personalised remote health monitoring applications

Sidharth Maheshwari[a], Amit Acharyya[b], Paolo Emilio Puddu[c] & Michele Schiariti[c]
[a] Electronics and Electrical Engineering, Indian Institute of Technology Guwahati, Guwahati 781039, Assam, India
[b] Department of Electrical Engineering, Indian Institute of Technology Hyderabad, Hyderabad, AP, India
[c] Department of Cardiovascular Sciences, Sapienza University of Rome, Rome, Italy
Published online: 27 Jan 2014.

To cite this article: Sidharth Maheshwari, Amit Acharyya, Paolo Emilio Puddu & Michele Schiariti (2014) Reduced lead system selection methodology for reliable standard 12-lead reconstruction targeting personalised remote health monitoring applications, Computer Methods in Biomechanics and Biomedical Engineering: Imaging & Visualization, 2:2, 107-120, DOI: 10.1080/21681163.2013.859097

To link to this article: http://dx.doi.org/10.1080/21681163.2013.859097

Computer Methods in Biomechanics and Biomedical Engineering: Imaging & Visualization, 2014
Vol. 2, No. 2, 107–120, http://dx.doi.org/10.1080/21681163.2013.859097

Reduced lead system selection methodology for reliable standard 12-lead reconstruction targeting personalised remote health monitoring applications

Sidharth Maheshwari[a1], Amit Acharyya[b2], Paolo Emilio Puddu[c*] and Michele Schiariti[c3]

[a]*Electronics and Electrical Engineering, Indian Institute of Technology Guwahati, Guwahati 781039, Assam, India;* [b]*Department of Electrical Engineering, Indian Institute of Technology Hyderabad, Hyderabad, AP, India;* [c]*Department of Cardiovascular Sciences, Sapienza University of Rome, Rome, Italy*

(*Received 10 May 2013; accepted 22 October 2013*)

Advanced wireless technology, high speed internet facility and availability of other communication systems can be used to provide the accessibility of state-of-the-art healthcare facilities to the patients in remote and rural areas for monitoring and diagnosis of cardiovascular diseases, one of the prime causes of human mortality today. Telemonitoring applications encounter technological constraints viz. bandwidth, storage and data transmission time due to which reduced lead (RL) ECG systems (containing three to four leads) are used. From the medical science perspective, cardiologists are accustomed to the standard 12-lead (S12) ECG system owing to its wide-spread acceptability and decades-long usage and these RL systems may prove to be insufficient for diagnosis. In this paper, we attempt to provide for the first time, to the best of our knowledge, a technical methodology to the medical practitioners for selection of such RL systems suitable for personalised remote health monitoring applications. Subsequently, a novel S12-lead ECG reconstruction methodology is also proposed which is shown to be more reliable than the state-of-the art lead reconstruction methodologies. In this study, along with Frank's vectorcardiographic system, reduced 3-lead systems consisting of leads I, II and one of the six precordial leads (V_1–V_6) leading to a total of six such reduced lead sub-systems are considered. Based on the proposed lead reconstruction methodology, these aforementioned reduced lead systems' performance are evaluated and compared comprehensively using R^2 statistics, correlation and regression coefficients. Furthermore, comparison of ECG features extracted from the original and reconstructed standard leads from each of these reduced lead systems by our recently proposed time domain morphology and gradient algorithm using root mean square error has been reported and discussed. The advantages and disadvantages of using a particular RL system have been discussed in the context of remote health monitoring applications.

Keywords: ECG; VCG; lead reconstruction; standard 12-lead system; Frank system; personalised remote healthcare

Abbreviations: ECG, electrocardiography; VCG, vectorcardiography; FV, Frank vectorcardiography system; S12, standard 12-lead system; RL, reduced lead system; R3L, reduced 3-lead system; PRHM, personalised remote health monitoring; CR, compression ratio; FRM, first reconstruction methodology; SRM, second reconstruction methodology; BW, baseline wandering; LS, least-square; DT, Dower transform

1. Introduction

In this paper, we attempt to provide a technical methodology to the medical practitioners for the selection of appropriate reduced lead (RL) system targeting personalised remote health monitoring (PRHM) applications for electrocardiography (ECG) acquisition by selecting two popular RL systems (discussed later in this section) and by comparing the performance extensively in terms of reconstructed standard 12-leads (S12) obtained from both of these RL systems using our proposed methodology (see Section 3). The two RL systems used to reconstruct S12 system are (1) Frank vectorcardiographic (FV) system and (2) six reduced 3-lead (R3L) system constituted by lead I, II and one of the six precordial leads i.e. V_1–V_6. The advantages and disadvantages of using a particular RL system for PRHM Applications have been discussed, and the factors which can govern the selection of a particular system have been mentioned.

Cardiovascular diseases (CVD) is one of the main causes of human mortality around the world (World Health Organisation 2009) which has led to tremendous research in the field of its detection and prevention. There are commercial products available which allow patients to stay at home and still be connected to ECG monitors (Liszka et al. 2004) using wireless technology, telephone or internet. These advancements focus on bringing relief and convenience to the patients suffering from cardiologic disorders by allowing them to stay at home or work still being monitored continuously through wireless transmission of signals to nearby state-of-the-art facility where they have been registered (Liszka et al. 2004). These developments in telemonitoring and telemedicine have greatly improved the quality of healthcare services; however, they are mainly limited to developed countries and urban areas (Prasad 2008). In developing countries, there is a need for implementation of these remote health

*Corresponding author. Email: paoloemilio.puddu@uniroma1.it

monitoring services (Prasad 2008) due to the large number of patients, scarcity of medical practitioners and caregivers, and more importantly the lack of basic healthcare infrastructure (Chudi 2010).

With the advancements in wireless technology, it has now become possible to connect rural and remotely accessed areas and provide availability and accessibility to state-of-the-art facilities in the urban areas for diagnosis and therapy. Implementation of such remote health monitoring system to cater to large number of patients in rural and remote areas will encounter two major problems from the technical and medical science perspective: first, limitations on bandwidth, storage capacity and data transmission time (Liszka et al. 2004; Brechet et al. 2007; Alesanco and Garcia 2008) and second, it is a standard clinical practice to examine S12 ECG, owing to its usage over decades and widespread acceptability, as a preliminary step in the diagnosis of CVD by the cardiologists and at times they may find other RL systems inadequate or insufficient for diagnosis, therapy and disease prognosis (Hoekema et al. 1999). The technological limitations can be allayed by using a RL system essentially with three to four leads, and the S12 system can be reconstructed for diagnosis by the cardiologists using lead reconstruction methodologies.

In this paper, we envisage a remote health monitoring scenario in which a patient is registered to a nearby state-of-the-art health centre which maintains a data repository to keep track of patient's health. The patients may belong to the region under the catchment area of the health centre or may be from a rural/remote area. During the registration process, a patient's ECG is acquired and transformation coefficients are generated which are stored along with the patient's database. In future, whenever the patient is monitored, the ECG signals from the RL system are transmitted to the health centre and S12 system is reconstructed using personalised reconstruction methodology which can be further displayed on cardiologists mobile phone/PDA/Tablet. From a technological perspective as of now, the main thrust of research has been on the communication module (Alesanco and Garcia 2010; Yu et al. 2012) and the signal processing module comprising of feature extraction (Mazomenos, Biswas, et al. 2013; Mazomenos, Chen, et al. 2012), irregular ECG wave pattern identification including Arrhythmia (Liu et al. 2013), wearable non-contact ECG sensing and acquisition system design (Yoo et al. 2009; Peng and Bocko 2013), cardiogram analysis and interpretation (He and Wu 2001; Rieta et al. 2004; Yang 2011) and signal compression (Brechet et al. 2007; Alesanco and Garcia 2008; Sharma et al. 2012). Algorithms for automated cardiogram interpretation and feature extraction have been developed for both remote and hospital-based environments to help cardiologists with proper diagnosis, therapy and prognosis of the disease. The signal compression techniques have been developed to address the storage and bandwidth issues; however, it should be noted that the compression ratio (CR) of these algorithms depend on the number of ECG channels (Sharma et al. 2012). The greater the number of channels, the lower is the CR; thus, a RL system can significantly improve the performance of these algorithms. Lead reconstruction methodologies have mostly been investigated in order to address the problems faced by patients and caregivers in hospital-based environments (Dower 1968; Dower et al. 1988; Nelwan et al. 2000; Nelwan, Kors, et al. 2004; Nelwan, Carter, et al. 2004; Finlay et al. 2007; Gregg et al. 2008; Dawson et al. 2009); however, they have not been evaluated in the context of remote health monitoring applications. Using a RL system for PRHM applications will require selection of an appropriate RL system. If proper methodology is available from the technical aspects, then cardiologists after considering other non-technical i.e. medical science aspects can accurately select the RL system relevant for a particular patient. This has been our motivation behind this work.

Two different lead reconstruction methodologies have been investigated in this paper. The first reconstruction methodology (FRM) involves transformation of six R3L systems which is comprised of leads I, II and one of the six precordial leads (V_1–V_6) to S12 system, and the second reconstruction methodology (SRM) involves transformation of FV (X, Y and Z) system to S12 system. A total of 275 patients from PhysioNet's PTB database (PTBDB) (Bousseljot et al. 1995; Goldberger et al. 2000) were categorised, on the basis of cardiologic disorders, and used in this investigation. ECG and VCG of each patient, after baseline wandering (BW) removal and denoising, were used to obtain personalised transformation coefficients employing least-square (LS) fit technique on the heart model proposed by heart-vector projection theory (Frank 1954; Dower 1968; Levkov 1987). The reconstructed signals were then compared with the original signal using R statistics, Correlation (b) and regression (r) coefficients. Pertaining to the omnipresence of computerised ECG acquisition and interpretation, we have employed our recently proposed domain morphology and gradient (TDMG) (Mazomenos, Chen, et al. 2012) algorithm to extract features from PQRST complexes of both originally measured and the reconstructed signal and computed root mean square error (RMSE) to provide a detailed comparative study and discuss efficiency of lead reconstruction methodologies for applications of automated ECG interpretation algorithms on reconstructed signals for RHM applications.

The paper is organised in the following manner. Section 2 presents the previous work on lead reconstruction, Section 3 presents the proposed methodology, Section 4 presents the results and discussions and Section 5 concludes the paper.

2. Previous work

Vectorcardiogram (VCG) represents the electrical activity of heart three-dimensionally as the components of a dipole vector (known as heart vector, $\vec{H} = X\hat{i} + Y\hat{j} + Z\hat{k}$) on the orthogonal planes (horizontal, frontal and sagittal) (Riera et al. 2007). VCG is useful in the 3D-visualisation of heart, diagnosis of certain diseases including myocardial ischemia, inferior myocardial infarction, Brugada syndrome, etc. and it captures the important characteristics of heart as good as the 12-lead ECG (Edenbrandt and Pahlm 1988; Riera et al. 2007; Vullings et al. 2010; Yang 2011). The most widely accepted system for VCG is the FV system (Li and Lin 2009). However, as mentioned earlier, cardiologists are accustomed to conventional 12-lead ECG (S12), and hence several lead transformation methodologies were proposed to transform an RL system to S12 system. Dower proposed a transformation matrix, popularly known as Dower transform (DT) in medical science, to transform FV system to S12 system (Dower 1968). Recently in (Dawson et al. 2009) the transformation matrix obtained using LS fit method applying on a population of patients (known as population based transformation matrix) outperformed DT. EASI system to S12 system is another transformation proposed which uses LS fit method and/or DT (Dower et al. 1988). Other population-based and patient-specific transformation reported in (Nelwan et al. 2000; Nelwan, Crater, et al. 2004; Nelwan, Kors et al. 2004; Gregg et al. 2008) reduce the inconvenience of patient and the caregiver during bedtime monitoring by reconstructing the missing precordial leads (which will be referred to as R3L systems from hereafter). Finlay et al. (2007) posit that the transformation involving reconstruction of missing precordial leads of S12 has been shown to outperform the transformation of EASI system to S12 system.

However, to the best of our knowledge, this is the first work which compares the performance of personalised or patient-specific transformation of FV to S12 and R3L to S12 systems. R3L system consists of three basis leads which is a subset of S12 system, consisting of one precordial lead along with leads I and II invariably present in all R3L systems. FV systems consists of heart-vector ($\vec{H}$) components as the basis leads, i.e. X, Y and Z. The target leads in this case are the 12 leads of the S12 system. As evident from the literature, personalised reconstruction has outperformed all other types of reconstruction strategies, and hence has been adopted in this investigation for accurate and reliable lead reconstruction.

3. Proposed methodology

Here, Section 3.1 discusses the envisaged remote health monitoring environment. The patients in PTBDB were categorised on the basis of their cardiologic disorders (Section 3.2). The raw signal was then preprocessed for removal of BW and noise (Section 3.3). Transformation coefficients were generated from the preprocessed signal using the classical heart model following the heart-vector projection theory and LS fit technique (Section 3.3). The reconstructed signals were then compared with the originally measured signals using various evaluation metrics (Sections 3.4 and 3.5).

3.1 Envisaged remote health monitoring scenarios

Figure 1 shows the two possible ways in which a patient can be registered at the health centre. During the registration process, the transformation coefficients are generated which can be eventually used to reconstruct the S12 system. The first scenario shows the online registration process and second shows the offline registration process. By 'online' we meant that the patient needs not to be present in the hospital/health-centre physically. In this case, the RL or Frank leads can be captured and transmitted to the hospital/health-centre for reconstruction of standard 12-leads. By 'offline' we meant

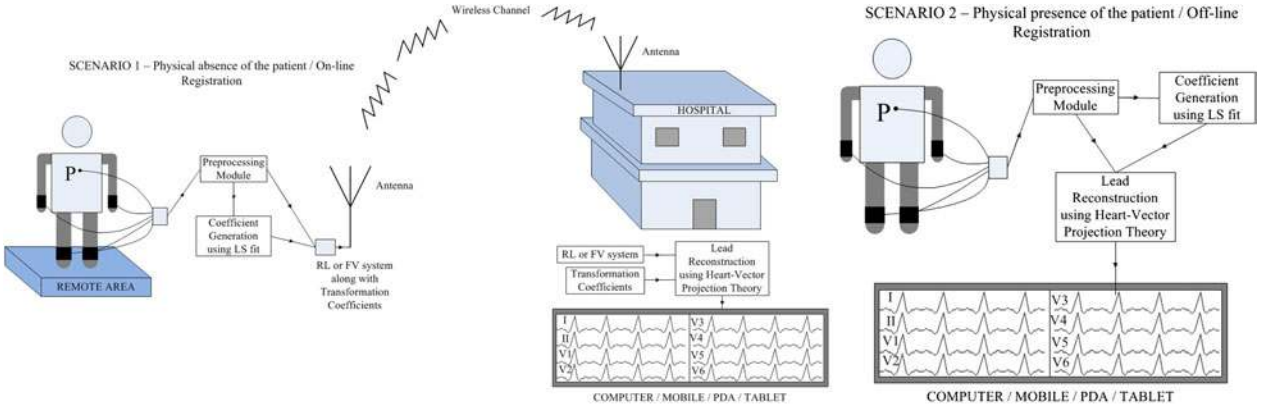

Figure 1. Envisaged remote health monitoring scenarios: (1) when patient may not be physically present for registration (online) and (2) when patient is available for registration (offline).

that the patient is present in the hospital/heath-centre physically. In this case, standard 12-lead reconstruction is done at the hospital/health-centre itself.

The aforementioned remote health monitoring service can benefit both ambulatory patients and the patients living in rural or remotely accessed areas. The following section discusses the registration process in the context of RL system used.

3.1.1 R3L systems to S12 system

If the reconstruction methodology being adopted is the transformation of R3L systems to S12 system, then for coefficient generation the acquisition of only S12 system is required. These coefficients can then be used to reconstruct S12 system on eventual readings.

3.1.2 FV system to S12 system

If the reconstruction methodology being adopted is the transformation of FV to S12 system, then for the coefficient generation a simultaneous acquisition of both the systems is required. On eventual monitoring, only FV system's acquisition is required which can be then transformed to S12 system.

3.2 Material

PTBDB (Goldberger et al.) is a 290-patient 15 lead database with both S12 and FV system simultaneously acquired and digitised at the sampling frequency of 1 kHz. Of the 290 patients, 275 were used and the rest were excluded from the study pertaining to their extreme artifacts and paced rhythm in consultation with the cardiologists. For all the patients in the database first recordings were used in this paper. The patients were divided on the basis of their cardiologic disorder into six categories viz. bundle branch block (BB – 14), healthy control (HC – 51), hypertrophy, cardiomyopathy and heart failure (HY – 24), myocardial infarction (MI – 140), valvular myocarditis and other miscellaneous (VA – 27) and patients with no diagnostic data (ND – 19).

3.3 Proposed lead reconstruction methodology

The 15-lead raw ECG of every patient is passed through a preprocessing module (Section 3.3.1) comprising of BW removal and denoising. After preprocessing, LS fit technique is used to obtain the personalised coefficients (section 3.3.2) for lead transformation and then the reconstructed leads are compared to original leads using various evaluation metrics (Sections 3.4 and 3.5).

3.3.1 Preprocessing module

Here, we propose a preprocessing module comprising of BW removal based on discrete wavelet transform (Zhang 2005) and denoising based on translation invariant wavelet transform (TIWT) (Zhang 2005). Figure 5 in Appendix provides the snippet of the MATLAB code for implementation of the preprocessing module to encourage the reproducible research. This code may also lead to the mobile-app development and validating the methodology proposed in this paper.

Other denoising methods (Hernandez and Olvera 2009; Li and Lin 2009) were also used however; TIWT was found to outperform the rest and therefore we used it in the proposed methodology. The implementation of TIWT requires the input number of samples to be in the power of 2. For example, if a patient's ECG is recorded for about 38 s, the number of samples obtained at a sampling rate of 1 kHz was 38,399, and out of these we have taken $2\wedge15 = 2{,}768$ samples i.e. first 32,768 samples for the algorithmic need and rest were excluded from the study. For every patient, the recording was reduced to the maximum power of 2 that can be accommodated in the original recording and was then used for all further processing throughout the work. For BW, the level of decomposition was down to level 9 and the wavelet used was Symmlet 10. For denoising, the level of decomposition was self-determined by the code, the wavelet used was symmlet 8 and hard thresholding was used.

3.3.2 Generation of transformation coefficients

Heart-vector projection theory (Levkov 1987; Zhang 2005) states that heart can be approximated as single dipole vector (known as heart vector, $\vec{H}$) fixed in 3-D space whose orientation and magnitude varies during a cardiac cycle. This dipole vector is responsible for the body surface potential observed when electrodes are placed on the body. The potential at any point on the body is the projection of $\vec{H}$ on the lead vector ($\vec{L}$) which is assumed to originate from the zero-potential region in the heart and terminates on the point located on the body (1).

$$V = \vec{H}\cdot\vec{L} = a_1X + b_1Y + c_1Z, \tag{1}$$

where $\vec{H} = X\hat{i} + Y\hat{j} + Z\hat{k}$ and $\vec{L} = a_1\hat{i} + b_1\hat{j} + c_1\hat{k}$. The linearity of the model can be used to obtain potential at any point using leads other than the heart vector components (X, Y and Z) as shown in (2).

$$V = a_2I + b_2II + c_2V_i. \tag{2}$$

In (2) we have used leads I, II and V_i (where $i = 1–6$ denotes a precordial lead) to generate the signal of some other lead. It can be seen from (1, 2) that any lead of S12 system can be generated from any other set of three independent leads, provided the coefficients are available. These coefficients can be generated statistically using LS fit technique upon the availability of leads appearing on right hand side and left hand side of (1, 2). The solution of

LS fit when applied to $V = a_i l_1 + b_i l_2 + c_i l_3$ is given by (3).

$$\begin{bmatrix} a_i \\ b_i \\ c_i \end{bmatrix} = \begin{bmatrix} \Sigma l_1^2 & \Sigma l_1 \cdot l_2 & \Sigma l_1 \cdot l_3 \\ \Sigma l_1 \cdot l_2 & \Sigma l_2^2 & \Sigma l_2 \cdot l_3 \\ \Sigma l_1 \cdot l_3 & \Sigma l_2 \cdot l_3 & \Sigma l_3^2 \end{bmatrix}^{-1} \begin{bmatrix} \Sigma V \cdot l_1 \\ \Sigma V \cdot l_2 \\ \Sigma V \cdot l_3 \end{bmatrix}, \quad (3)$$

where l_1, l_2 and l_3 are any three leads and a_i, b_i and c_i are the respective coefficients. These coefficients are used to transform a set of leads to another lead signal and hence are known as transformation coefficients. When LS fit method is applied on one patient, the coefficients obtained are personalised or patient-specific, and when applied on a group of patients are known as population-specific coefficients. A training set of 5000 samples from the middle of the recording of each patient was used in (3) for obtaining the transformation coefficients and the whole recording was used as the testing set. The complete work was carried out on MATLAB (Version 7.10.0.499 R2010a).

3.4 Evaluation metrics

R^2 statistics, correlation coefficient, regression coefficient (Levkov 1987; Dawson et al. 2009) and RMSE have been used as performance evaluation metric. R^2 statistics has been used to evaluate the degree of association between the measured and the reconstructed signal. Perfect retracing of the measured wave by the reconstructed wave will be indicated by a value 100%. Correlation coefficient (r_x) (Levkov 1987) is a metric to estimate the similarity between the two signals, and regression (b_x) (Levkov 1987) fairly estimates the amplitude differences between the measured and reconstructed signal. RMSE is a good measure for accuracy.

$$R^2 = \left\{1 - \frac{\Sigma[\text{Derived(sample}\,k) - \text{Measured(sample}\,k)]^2}{\Sigma[\text{Measured(sample}\,k)]^2}\right\} \times 100, \quad (4)$$

$$r_x = \left\{\frac{\Sigma(\text{Measured sample}\,i) \times (\text{Derived sample}\,i)}{(\Sigma(\text{Measured sample}\,i)^2 \times \Sigma(\text{Derived sample}\,i)^2)^{1/2}}\right\}, \quad (5)$$

$$b_x = \left\{\frac{\Sigma(\text{Measured sample}\,i) \times (\text{Derived sample}\,i)}{\Sigma(\text{Measured sample}\,i)^2}\right\} \quad (6)$$

$$\text{RMSE} = \sqrt{\frac{\sum_{i=1}^{n}\left(x_i - x_j\right)^2}{n}} \quad (7)$$

.

3.5 Detailed comparison of ECG features of reconstructed and original signal

TDMG (Mazomenos, Chen, et al. 2012) operates accurately on a single heart beat. However, it is not feasible to manually detect and select a PQRST complex from all the 12 leads of 275 patients for both original and reconstructed signals using all the RL systems (in total 7), which accounts to a total of 57,750 lead evaluations. To automate the process of annotation and selection of PQRST complex, we used the help of two open source MATLAB files viz. *nqrsdetect·m* (Afonso et al. 1999) and *select_train · m* (http://www.robots.ox.ac.uk/ gari/CODE/ECGtools/). The former function detects the fiducial points of QRS complexes. The latter function has been used for the extraction of PQRST complexes through variations in the input arguments. To attain this complex task, the PQRST complexes of each patient in all the categories were visually observed to fine tune the input arguments so that only one complete heart beat is extracted and TDMG algorithm is

Table 1. Denotations of R3L systems and various ECG features extracted using TDMG algorithm.

Basis leads of RL system	Denotation	ECG features (unit)	Denotation
I, II, V_1	**I**	*P* duration (ms)	**1**
I, II, V_2	**II**	*P* height (μV)	**2**
I, II, V_3	**III**	PR interval (ms)	**3**
I, II, V_4	**IV**	PR segment (ms)	**4**
I, II, V_5	**V**	*Q* peak (μV)	**5**
I, II, V_6	**VI**	QRS length (ms)	**6**
Frank Leads *X*, *Y* and *Z*	**FV**	QT interval (ms)	**7**
		R height (μV)	**8**
		S peak (μV)	**9**
		ST interval (ms)	**10**
		ST segment (ms)	**11**
		T duration (ms)	**12**
		T height (μV)	**13**

Table 2. Mean R^2, r_x and b_x values of various categories for the transformation of RL systems (V_1–V_6: I–VI) to S12 systems.

		V_1			V_2			V_3			V_4			V_5			V_6			
		R^2	r_x	b_x	R^2	r_x	b_x	R^2	r_x	b_x	R^2	r_x	b_x	R^2	r_x	b_x	R^2	r_x	b_x	Avg
BB	**I**	100	1	1	83.36	0.91	0.872	79.93	0.9	0.865	80.54	0.91	0.886	87.64	0.938	0.909	92.59	0.963	0.945	93.07
	II	90.4	0.947	0.899	100	1	1	95.78	0.979	0.975	87.39	0.937	0.913	88.47	0.944	0.919	92.41	0.962	0.952	95.6
	III	87.05	0.929	0.864	95.07	0.975	0.942	100	1	1	94.16	0.971	0.965	89.36	0.949	0.93	92.25	0.962	0.952	95.89
	IV	84.68	0.919	0.849	77.53	0.873	0.779	89.47	0.943	0.896	100	1	1	91.6	0.963	0.954	92.03	0.962	0.951	94
	V	78.24	0.889	0.815	64.08	0.798	0.688	67.28	0.813	0.728	74.2	0.848	0.805	100	1	1	94.24	0.971	0.963	89.23
	VI	83.18	0.911	0.832	71.52	0.847	0.757	73.5	0.867	0.804	76.13	0.885	0.839	91.15	0.954	0.913	100	1	1	90.69
HC	**I**	100	1	1	94.57	0.972	0.947	93.51	0.967	0.935	93.14	0.965	0.936	95.29	0.976	0.957	96.82	0.984	0.972	97.76
	II	95.79	0.978	0.959	100	1	1	97.3	0.986	0.975	94.29	0.971	0.948	95.54	0.978	0.959	97.01	0.985	0.974	98.31
	III	92.17	0.958	0.924	95.55	0.978	0.961	100	1	1	96.77	0.984	0.97	96.11	0.98	0.963	96.81	0.984	0.972	98.1
	IV	82.23	0.901	0.827	80.59	0.888	0.816	92.57	0.962	0.93	100	1	1	97.66	0.988	0.978	96.6	0.983	0.969	95.79
	V	73.18	0.846	0.74	66.38	0.794	0.678	77.04	0.868	0.777	92.18	0.959	0.924	100	1	1	97.78	0.989	0.981	92.2
	VI	78.49	0.878	0.795	74.56	0.857	0.764	79.04	0.885	0.801	87.66	0.935	0.883	96.92	0.984	0.969	100	1	1	93.04
HY	**I**	100	1	1	96.15	0.98	0.962	90.83	0.953	0.921	85.62	0.925	0.883	89.13	0.939	0.893	95.39	0.976	0.953	96.41
	II	97.44	0.987	0.979	100	1	1	96.23	0.981	0.968	87.45	0.934	0.897	89.9	0.945	0.899	95.74	0.978	0.957	97.22
	III	95.58	0.978	0.961	97.3	0.987	0.972	100	1	1	93.52	0.966	0.949	91.61	0.955	0.918	95.98	0.979	0.958	97.82
	IV	91.88	0.958	0.925	88.94	0.941	0.888	93.48	0.967	0.93	100	1	1	94.45	0.971	0.941	96.63	0.983	0.962	97.1
	V	85.25	0.921	0.861	78.51	0.878	0.797	77.9	0.883	0.796	86.81	0.929	0.887	96.91	0.984	0.967	100	1	1	93.77
	VI	84.73	0.916	0.855	77.05	0.861	0.778	70.86	0.83	0.721	74.65	0.842	0.76	90.32	0.947	0.906	100	1	1	91.45
MI	**I**	100	1	1	92.1	0.958	0.923	87.73	0.935	0.88	84.07	0.914	0.844	87.56	0.934	0.875	91.19	0.954	0.907	95.2
	II	94.34	0.971	0.947	100	1	1	95.92	0.979	0.959	89.52	0.945	0.895	89.22	0.944	0.889	91.52	0.956	0.911	96.69
	III	89.82	0.946	0.907	95.35	0.976	0.959	100	1	1	95.55	0.977	0.954	91.49	0.956	0.912	91.64	0.956	0.913	96.96
	IV	82.21	0.903	0.834	83.34	0.909	0.844	92.55	0.96	0.93	100	1	1	94.84	0.974	0.947	91.83	0.958	0.915	95.37
	V	73.83	0.852	0.75	68.54	0.818	0.701	73.96	0.851	0.753	84.38	0.907	0.85	100	1	1	94.72	0.973	0.946	91.26
	VI	73.93	0.851	0.752	64.98	0.786	0.666	65.35	0.796	0.67	70.35	0.826	0.714	89.99	0.947	0.905	100	1	1	88.69
VA	**I**	100	1	1	90.63	0.95	0.901	86.57	0.929	0.866	85.54	0.924	0.863	91.6	0.957	0.917	93.74	0.968	0.934	95.63
	II	93.73	0.967	0.942	100	1	1	94.25	0.97	0.945	89.97	0.948	0.906	91.89	0.959	0.921	93.78	0.968	0.934	96.93
	III	88.68	0.935	0.888	92.86	0.961	0.927	100	1	1	95.84	0.979	0.96	93.79	0.968	0.968	94.27	0.97	0.937	97.08
	IV	81.68	0.895	0.817	80.38	0.889	0.801	91.69	0.957	0.913	100	1	1	93.96	0.963	0.941	94.89	0.974	0.945	95.18
	V	74.11	0.834	0.748	68.59	0.816	0.691	77.72	0.877	0.779	90.66	0.95	0.908	100	1	1	97.14	0.985	1	92.31
	VI	78.02	0.874	0.782	69.18	0.819	0.692	72.02	0.841	0.723	80.46	0.888	0.816	96.02	0.979	0.967	100	1	1	91.27
ND	**I**	100	1	1	90.42	0.951	0.916	81.28	0.891	0.825	78.06	0.876	0.787	82.08	0.902	0.823	85.84	0.91	0.86	92.39
	II	90.92	0.949	0.913	100	1	1	93.54	0.967	0.931	83.72	0.91	0.838	84.61	0.916	0.847	87.28	0.92	0.876	94.44
	III	88.18	0.937	0.899	95.74	0.978	0.963	100	1	1	93.07	0.965	0.931	88.5	0.939	0.887	88.4	0.932	0.89	96.02
	IV	83.27	0.911	0.856	83.5	0.914	0.857	90.22	0.95	0.916	100	1	1	95.58	0.977	0.952	92.85	0.963	0.928	95.39
	V	76.77	0.874	0.796	68.32	0.825	0.723	67.11	0.802	0.704	90.12	0.948	0.909	100	1	1	96.89	0.984	0.969	91.52
	VI	78.51	0.883	0.816	72.83	0.853	0.766	69.69	0.831	0.728	83.32	0.911	0.843	94.97	0.974	0.951	100	1	1	91.51

Note: Average value shown has been taken from all the 12 leads.

successfully operational on all of them. The arguments were needed to be changed for different categories. A minimum of five PQRST complexes were averaged and then were operated upon by the TDMG algorithm; similarly, the corresponding complexes in the reconstructed signals were averaged and TDMG was then applied on them. ECG is approximately a periodic signal; however, while traversing through the leads it was found that some PQRST complexes were distorted in shape significantly compared to the adjacent complexes, and hence for evaluation if these particular complexes were selected, they may lead to unreliable and inaccurate results. Hence, the mean was obtained over a minimum of five complexes before applying TDMG. The results obtained for the original and reconstructed signal from the TDMG algorithm were then compared using RMSE. Figure 6 in Appendix presents the MATLAB code snippet for the implementation of all the three aforementioned functions i.e. *nqrsdetect·m*, *select_train·m* and *tdmg·m*.

4. Results and discussion

In this section, we attempt to provide a detailed examination of the quality of reconstruction obtained from various RL systems. The 12 leads of the S12 system have been divided into two lead sets: set 1 comprises of leads I, II, III, aVR, aVL, aVF and set 2 comprises of the precordial leads. The FRM involves a total of six R3L system and SRM involves one, i.e. FV system; therefore, a total of seven RL systems. Table 1 shows the denotations of these seven RL systems. We have used '**I**', '**II**', etc. in bold letters to denote R3L systems with precordial leads V_1, V_2, etc. as the basis leads in the R3L systems, respectively (Table 1). FV system has been denoted by **FV** in bold. Table 1 also shows the denotations of 13 different features that were extracted using TDMG for comparison starting from **1** to **13** in bold letters.

Table 2 presents the mean R^2, correlation and regression coefficient values of the FRM i.e. R3L systems to S12 system for the reconstruction of lead set 2. The last column of Table 2 shows the mean R^2 values over all the 12-leads of patients in the corresponding categories using FRM. As leads I and II are involved in the basis lead sets of all the six R3L systems, the resulting R^2, r_x and b_x values of lead set 1 when FRM is used are 100%, 1.0 and 1.0, respectively. Better results have been obtained when the precordial lead in the basis lead set are V_2 or V_3 followed by V_1 or V_4 and V_5 or V_6. The proximity effect as mentioned in (Feild et al. 2008) can be seen from the Table 2. Leads which are close to the basis leads have better reconstruction compared to those far from them. As for an illustration, row 1 of the 'BB' case in Table 2, basic lead of RL system i.e. **I** (comprising of lead I, II and V_1 as per the definition given in Table 1) is used to reconstruct

Table 3. Mean R^2, r_x and b_x values of various categories for the transformation of FV system to S12 system.

	BB			HC			HY			MI			VA			ND		
	R^2	r_x	b_x	R^2	r_x	b_x	R^2	r_x	b_x	R^2	r_x	b_x	R^2	r_x	b_x	R^2	r_x	b_x
I	90.89	0.952	0.898	95.99	0.98	0.96	95.34	0.976	0.959	92.41	0.961	0.93	94.15	0.971	0.955	93.61	0.968	0.927
II	94.29	0.97	0.944	99.04	0.995	0.99	98.33	0.992	0.983	96.54	0.982	0.967	97.41	0.987	0.982	93.55	0.966	0.947
III	88.29	0.916	0.88	93.18	0.965	0.929	95.41	0.976	0.952	93.55	0.967	0.94	91.99	0.958	0.918	91.84	0.952	0.92
aVR	91.06	0.953	0.914	98.49	0.993	0.985	97.71	0.989	0.979	93.86	0.969	0.945	95.59	0.978	0.966	91.6	0.955	0.918
aVL	91.05	0.953	0.904	91.75	0.957	0.918	93.63	0.967	0.937	92.18	0.96	0.926	90.28	0.945	0.914	94.24	0.971	0.963
aVF	96.01	0.98	0.961	98.09	0.99	0.98	97.34	0.987	0.974	95.99	0.979	0.96	96.41	0.982	0.966	95.6	0.977	0.959
V_1	91.12	0.954	0.897	96.41	0.982	0.966	97.29	0.986	0.977	94.15	0.97	0.949	94.83	0.974	0.953	92.07	0.959	0.928
V_2	89.31	0.943	0.89	94.03	0.97	0.942	96.39	0.982	0.961	92.29	0.96	0.929	91.19	0.951	0.916	91.28	0.955	0.925
V_3	94.44	0.973	0.953	96.9	0.984	0.968	96.91	0.985	0.971	94.56	0.972	0.95	95.2	0.976	0.959	94.72	0.973	0.953
V_4	93.75	0.97	0.961	98.06	0.99	0.982	95.82	0.979	0.974	95.66	0.977	0.959	97.36	0.987	0.984	97.04	0.985	0.967
V_5	97.79	0.989	0.976	99.27	0.996	0.993	96.19	0.98	0.964	97.53	0.988	0.975	98.8	0.994	0.991	96.64	0.983	0.964
V_6	98.7	0.994	0.991	99.51	0.998	0.996	99.24	0.996	0.992	97.54	0.988	0.974	98.74	0.994	0.988	98.12	0.991	0.983
Avg	93.06	0.9623	0.931	96.73	0.983	0.967	96.63	0.983	0.968	94.69	0.973	0.950	95.16	0.975	0.958	94.11	0.969	0.9436

V_1-V_6 in standard 12-lead ECG system. It is apparent from the row 1 that R^2, correlation (r_x) and regression (b_x) for the reconstruction of V_1 is 100%, 1 and 1 respectively; V_2 is 83.36%, 0.91 and 0.872, respectively and so on. In this way, all rows of Table 2 for different diseased classes as well as Healthy Control can be read and interpreted.

Table 3 shows the reconstruction results from SRM, i.e. FV to S12 system with average values mentioned in the last row. Figure 2 shows bar plots of mean R^2 values for lead set 1 (Figure 2(a)) and lead set 2 (Figure 2(b)). From Figure 2, we can see that FV system has consistently reconstructed all the leads, especially, the precordial leads. From Figure 2 along with Tables 2 and 3, it can be seen that the FRM outperforms SRM for lead set 1 as leads I and II constitute the basis lead set and other four dependent leads can be derived from them using simple linear algebraic relations. However, still second methodology produces more than 90% R^2 value for all these leads. For leads V_5 and V_6, second methodology (i.e. FV to S12) outperforms all others except where the same leads themselves form the basis leads. For rest of the four precordial leads, the performance of R3L systems are inconsistent compared to FV system.

The mean R^2 values of reconstruction of precordial leads (lead set 2) from R3L systems are **I**-91.24%, **II**-93.8735%, **III**-94.4031%, **IV**-91.1372%, **V**-83.4569%, **VI**-80.6942% and for **FV** system is 95.8141%. We can see that for lead set 2 SRM outperforms FRM. For lead set 1, it is ≈100% (FRM) versus 94.51% (SRM). The aforementioned mean values and the values used in Figure 2 were taken over the complete database (all 275 patients). The overall mean (taken over all the patients and 12 leads) R^2 values for R3L systems and FV system were: 95.52% (**I**), 96.85% (**II**), 97.14% (**III**), 95.51% (**IV**), 91.67% (**V**), 90.29% (**VI**) and 95.16% (FV), respectively.

Figure 3(a)–(c) present reconstructed signal (red) overlapping the original signal (blue), obtained using SRM, of three different patients with worst (71.3%), 80% and best case (99.61%) mean R^2 values for lead set 1. The R^2 values of corresponding leads are mentioned in the figure. The quality of reconstruction that a particular R^2 value corresponds can be observed from Figure 3. From Figure 3 we can see that when R^2 values are low, then except the QRS complex the rest of the original signal, i.e. P and T wave is almost completely retraced by the reconstructed signals. The main difference between the reconstructed and original signals with low R^2 values is that peaks and nadirs of QRS complexes are not accurately retraced, and this can also be seen from the comparison of features extracted from both the signals (discussed later in this section). Figure 3(d)–(i) presents a similar comparison for lead set 2 for both FRM and SRM, where the first six boxes in all the sub-figures correspond to FRM in the order of R3L systems with leads V_1, V_2, V_3, V_4, V_5 and V_6 as the precordial lead in the basis lead set and the last box corresponds to SRM. Figure 3(d) corresponds to reconstruction of V_1, similarly, Figure 3(e) corresponds to reconstruction of V_2 and so on.

Figure 4 provides the box plot of lead-wise mean RMSE for 13 different features extracted using TDMG over the complete database. Each sub-figure in Figure 4, i.e. a–h, presents 13 boxes numbered **1–13** each corresponding to a particular feature. The correspondence between the labels in the horizontal axis and features has been described in Table 1. Figure 4(a)–(f) follows from the reconstruction results of RL systems for lead set 2 with basis lead following the order: a–V_1, b–V_2, c–V_3, d–V_4, e–V_5 and f–V_6 (all of these basis lead sets essentially contain leads I and II). Figure 4(g),(h) follows from the results of SRM for lead set 2 and lead set 1, respectively. The edges of the box are the 25th and 75th percentiles, the

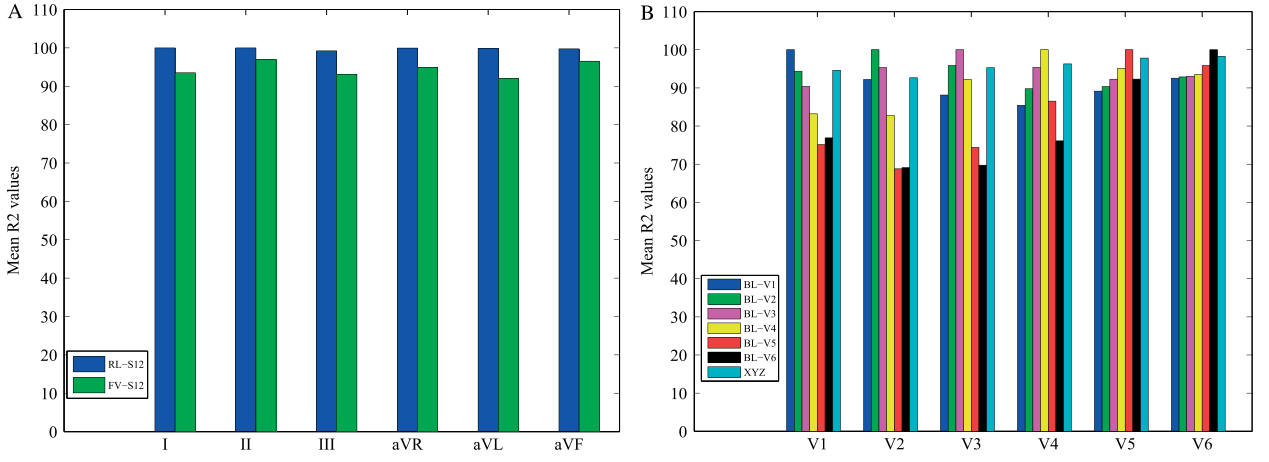

Figure 2. (Colour online) Bar plot of lead wise mean R^2 values. (a) RL to S12 (blue) versus FV to S12 (green) for lead set 1 i.e. I, II, III, aVR, aVL and aVF. (b) Comparison between all the seven reconstruction methodologies for reconstruction of precordial leads (lead set 2): leftmost to sixth bar correspond to RL systems with basis lead in the order V_1 (blue), V_2 (green), V_3 (magenta), V_4 (yellow), V_5 (red), V_6 (black) and the rightmost corresponds to FV (cyan) system, respectively.

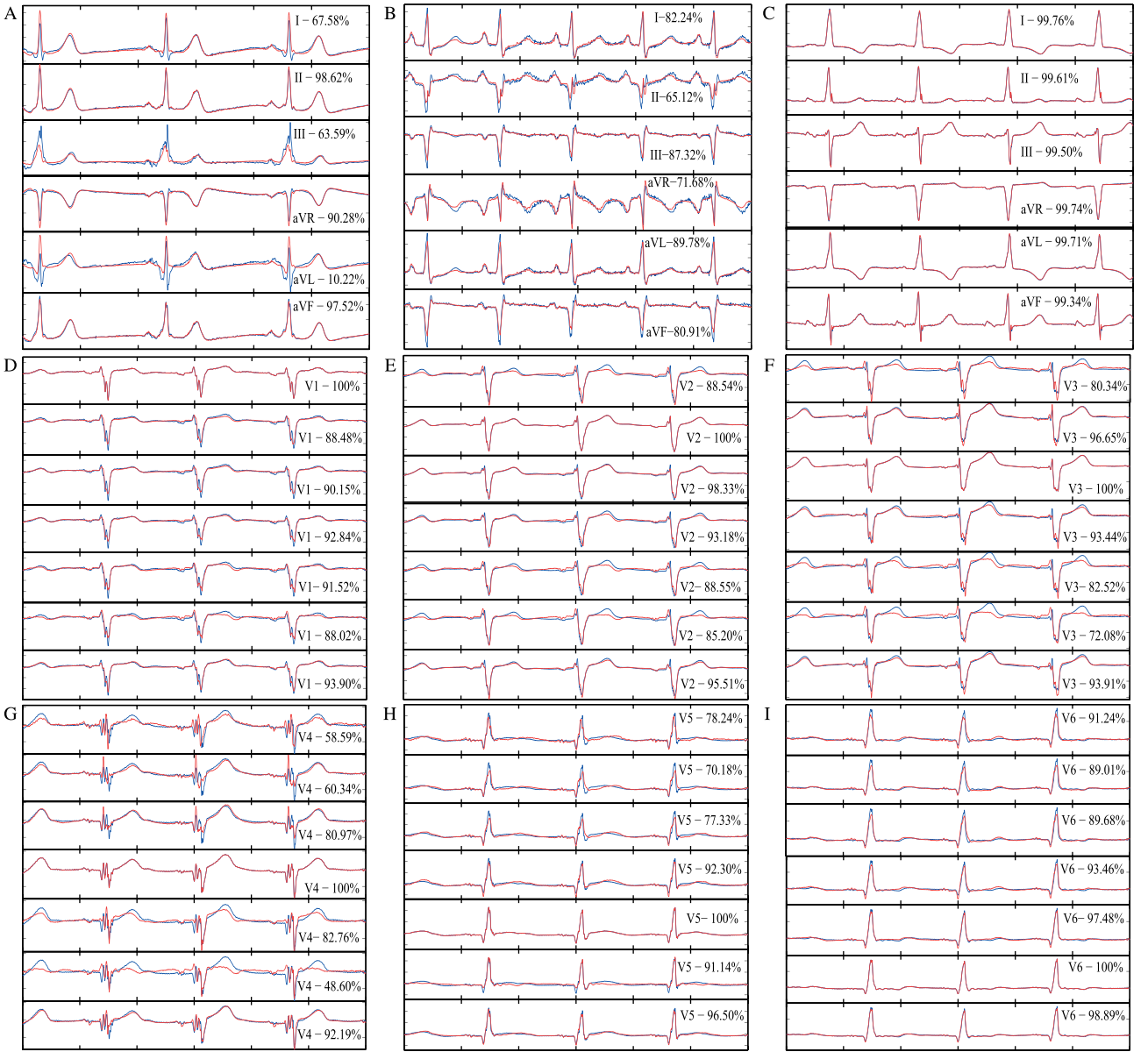

Figure 3. (Colour online) Comparison between the reconstructed (red) and the measured (blue) ECG signal. a–c Shows the reconstruction of lead set 1 using SRM, i.e. FV to S12 for the worst, 80% and the best case mean R^2 values. d–i show the reconstruction of lead set 2 (V_1–V_6) for all the RL systems with the basis leads starting from V_1 (top) to V_6 and FV system (bottom).

whiskers extend to ± 2.7 standard deviation (σ) and rest are plotted individually (http://www.mathworks.in/help/stats/boxplot.html). Table 4 provides the mean RMSE values for all the seven methodologies. It can be seen that higher values of error has mainly occurred when height or depth of a peak was measured in comparison to the features measuring the horizontal intervals. Among the R3L systems, R3L systems with basis leads V_2 and V_3 have outperformed the others. SRM has outperformed FRM for lead set 2; however, the results are otherwise for lead set 1.

The transformation coefficients depend on the following: position of electrodes, age, sex, size, shape, body fat distribution, homogeneity and several cardiac disorder faced by the patient (Feild et al. 2008). It can be realised that due to these factors, accurate and reliable lead reconstruction cannot be anticipated from population-based coefficients or DT (Dower 1968). Heart-vector projection theory considers an approximate and simplistic model of heart and hence the accuracy that can be achieved is limited. Furthermore, automated ECG interpretation algorithms are sensitive to minute changes which may be difficult to perceive through the human eye. Hence, all these limitations combined require a very accurate form of reconstruction which, as our results

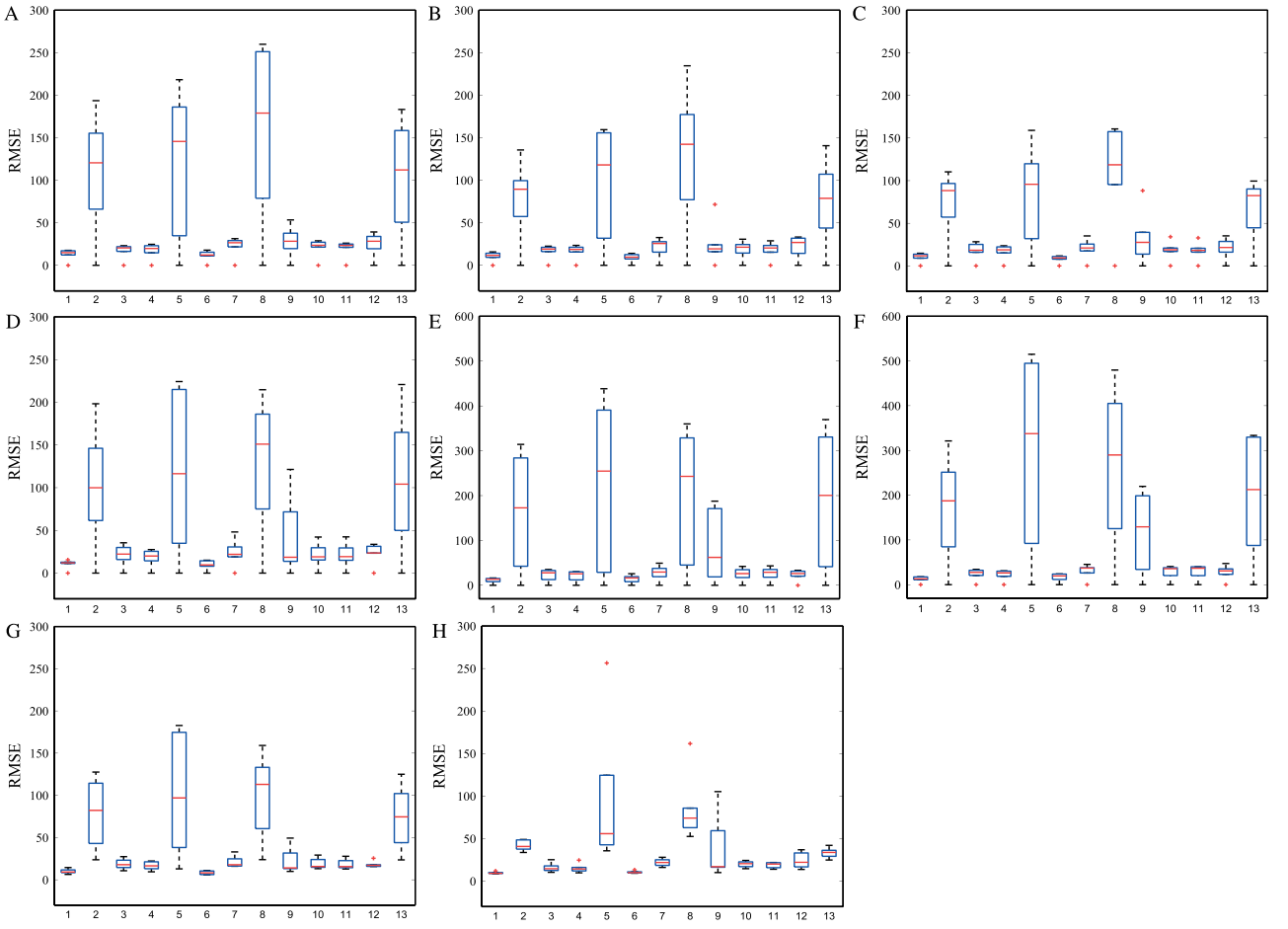

Figure 4. Box plot of RMSE values. Starting from left to right with R3L systems **I**–**VI** for lead set 2. The left sub-figure last row corresponds to lead set 2 and right sub-figure corresponds to lead set 1 when S12 was reconstructed from FV. The labels **1**–**13** on the horizontal axis corresponds to the respective features extracted from TDMG as mentioned in the text. For details about denotations, please refer Table 1.

present, can be achieved by Personalised Transformations (PT) using our proposed methodology. Let us consider that a patient who is registered in a hospital/ health-centre, whose standard 12-lead ECG has been obtained and coefficients are generated for the best suitable RL system in a personalised fashion using our proposed methodology, is diagnosed initially at the hospital/health-centre itself by the medical practitioners. This standard 12-lead ECG

Table 4. Mean RMSE values of the ECG features extracted using TDMG algorithm for all the RL systems.

Sr.	Feature (unit)	I	II	III	IV	V	VI	FV
1	*P* duration (ms)	6.700	5.536	5.423	5.644	5.888	6.357	9.750
2	*P* height (μV)	55.47	40.04	37.30	51.00	82.70	86.57	60.24
3	PR interval (ms)	9.058	8.639	9.281	10.96	11.80	12.27	17.20
4	PR segment (ms)	8.982	8.567	8.595	9.36	10.68	11.45	15.81
5	*Q* peak (μV)	63.60	51.33	44.34	61.49	116.4	150.6	97.75
6	QRS length (ms)	5.997	4.710	4.355	4.966	7.407	8.527	9.400
7	QT interval (ms)	11.97	11.26	10.64	12.41	14.38	15.98	21.41
8	*R* height (μV)	79.96	65.48	54.85	65.47	102.3	133.1	92.78
9	*S* peak (μV)	14.25	12.87	16.67	20.79	42.10	59.59	29.73
10	ST interval (ms)	10.94	9.889	9.629	10.94	12.69	14.72	19.32
11	ST segment (ms)	10.45	9.542	9.316	10.96	13.36	15.00	18.49
12	*T* duration (ms)	13.33	11.85	11.03	12.04	12.21	14.88	21.16
13	*T* height (μV)	52.42	38.26	33.79	54.17	95.76	98.51	53.61

Table 5. Comparison of FRM and SRM in context of remote healthcare applications.

	R3L system	FV system
1	Five electrodes	Eight electrodes
2	Three leads	Three leads
3	Inconsistent reconstruction of precordial leads.	Consistent reconstruction of precordial leads
4	Comparatively bad reconstruction of V_5 and V_6	Comparatively better reconstruction of V_5 and V_6
5	Leads I, II, III, aVR, aVL and aVF are obtained with approximately no information loss	Comparatively less accurate and information is lost in the reconstructed signal
6	Not much change in already existing acquisition system is required	A different system is required which can acquire both ECG and VCG
7	Online and offline registration possible	Online registration difficult
8	Only S12s are available and have to rely on inverse DT to obtain VCG which is inaccurate	Both VCG and ECG are present, and hence the advantages of VCG can be obtained directly

information is stored and maintained in the hospital as the patient's database. Afterwards, when remotely patients' ECGs are received from the prescribed RL system, these are first used to reconstruct the corresponding standard 12-lead ECG using our proposed methodology. This reconstructed ECG and the originally stored standard 12-lead ECG are compared using the evaluation metrics as shown in Section 3.4. If the performance is above the expected threshold, patients' health can be considered to be fine. If it falls below this threshold, this may raise an alarm at the medical practitioners' end so that proper and immediate personalised action can be initiated. Therefore, if the patient initially is diagnosed as 'normal', however he/she develops 'MI' type changes, and it will have an immediate impact on the performance of the reconstructed standard 12-lead ECG. Hence, this personalised approach will be able to give an immediate hint about the degradation of the patient health condition. Our results show that PT has produced 96.73% mean R^2 value as compared to 84.79% (Bousseljot et al. 1995) for HC subjects and 94.73% versus 80.77% (Nelwan, Kors, et al. 2004) for other patients when SRM was used (see Table 3). The mean correlation coefficient for the best lead subset as produced by (Bousseljot et al. 1995; Riera et al. 2007) is 0.983 versus 0.985 (for I, II and V_3) and 0.983 (for I, II and V_2) when FRM was used (see Table 2). The maximum value achieved by PT was 0.997 as compared to 0.990 (Bousseljot et al. 1995; Riera et al. 2007).

One important inference can also be drawn from the present study regarding the data compression as mentioned in Section 1. Assuming no sophisticated data-compression algorithm as proposed in (Brechet et al. 2007; Alesanco and Garcia 2008; Biswas et al. 2012; Sharma et al. 2012) is applied at the sensing, processing or data-transmission levels and given the number of samples per channel remains the same, if three channels are transmitted instead of 12 (corresponding to 12 leads), 75% compression is achieved. Under the same assumption, instead of sending all 12 channels, if only the eight channels (corresponding to eight independent leads viz. Lead I, II and 6 precordial leads V_1–V_6) are transmitted, then 62.5% compression is obtained. Therefore, just by reducing the number of leads to 3 and ensuring robust and reliable reconstruction of standard 12-lead ECG signals of medically acceptable quality at the receiver end using our proposed methodology, it is apparent that significant amount of compression can be achieved. It is therefore imperative to say that if the existing sophisticated data compression techniques are applied on these three channels, further compression can be accomplished.

5. Conclusion

This paper can be summarised as follows:

- Use of personalised transformations (PT) and a preprocessing module has considerably improved the reconstruction performance as shown in Section 4.
- This paper has presented a comprehensive comparison between transformations of RL systems involving FV and R3L systems to S12 system, to the best of our knowledge, for the first time.
- This paper has attempted to quantify the technical and non-technical difficulties that are, generally, encountered in all telemonitoring applications. Generally, ECG compression algorithms (Brechet et al. 2007; Alesanco and Garcia 2008; Sharma et al. 2012) are used to provide a solution to the technical problems; however, they have limitations which can be mitigated by using a RL system. The non-technical constraint can be mitigated using the proposed lead reconstruction technique.
- This work has enumerated the important parameters that will determine the selection of a particular RL system and provide a technical methodology for their selection.

With the help of Figure 3 and in consultation with the cardiologists, we assume that any reconstruction with more than 80% R^2 value can be considered to have significant diagnostic value and R^2 values more than 90% can be assumed to have high diagnostic value. Table 5 presents a comparison between FRM and SRM in the context of remote healthcare monitoring applications. Usinf FRM, lead positions V_5 and V_6 have comparatively underperformed. Among the R3L systems, usually lead positions

for V_3 and V_4 are avoided to leave the left chest open for bandaging, accessibility to defibrillator pads, echocardiography transducers and other non-ECG testings (Gregg et al. 2008). Hence, nontechnical factors suggest the usage of R3L system with basis lead V_2, which is also one of the most examined precordial lead. R3L systems also provide the flexibility of using any basis lead as per the suggestion of the cardiologist. FV system, on the other hand, can provide valuable information contained in both VCG and ECG and can help in the accurate and reliable diagnosis of the patient. A complete 3D visualisation of heart can provide important information regarding the condition of heart (Dawson et al. 2009; Yang 2011). VCG has been found to be better than S12 system in several diseases including myocardial ischemia, inferior myocardial infarction, Brugada syndrome, etc. (Bergmann and McGregor 2011; Correa et al. 2013). One of the major problems that lie in the implementation of FV system is the unconventional placement of electrodes, i.e. in the neck and back of the patient. However, this limitation can be mitigated by using wearable wireless sensors (Scanaill et al. 2006; Bergmann and McGregor 2011) which have been designed intending comfort of the patients. This paper proposes a solution to technical limitations of ECG acquisition using clinically accepted S12 system for PRHM applications by providing the flexibility of using one of seven RL systems, i.e. six R3L and FV system; however, the selection of appropriate RL system will be ultimately determined from the medical perspective of the cardiologists.

Funding

This work was supported by the DIT, India under the Cyber Physical Systems Innovation Hub [grant number 13 (6)/2010-CC&BT], Dated 01.03.11.

Notes

1. Email: m.sidharth@iitg.ac.in; sidharth.iitg@gmail.com
2. Email: amit_acharyya@iith.ac.in
3. Email: michele.schiariti@uniroma1.it

References

Afonso VX, Tompkins WJ, Nguyen TQ, Luo S. 1999. ECG beat detection using filter banks. IEEE Trans Biomed Eng. 46 (2):192–202.

Alesanco A, Garcia J. 2008. Automatic real-time ECG coding methodology guaranteeing signal interpretation quality. IEEE Trans Biomed Eng. 55(11):2519–2527.

Alesanco A, Garcia J. 2010. Clinical assessment of wireless ECG transmission in real-time cardiac telemonitoring. IEEE Trans Inf Technol Biomed. 14(5):1144–1152.

Antoniadis A, Bigot J, Sapatinas T. 2001. Wavelet estimators in nonparametric regression: a comparative simulation study. J Stat Softw. 6(6):1–83.

Bergmann JHM, McGregor AH. 2011. Body-worn sensor design: what do patients and clinicians want? Ann Biomed Eng. 39(9):2299–2312.

Biswas D, Mazomenos EB, Maharatna K. 2012. ECG compression for remote healthcare systems using selective thresholding based on energy compaction. International Symposium on Signals, Systems, and Electronics; 03–05 October 2012; Potsdam, DE.

Bousseljot R, Kreiseler D, Schnabel A. 1995. Nutzung der EKGSignaldatenbank CARDIODAT der PTB ber das Internet. Biomedizinische Technik. Band 40(Ergnzungsband 1):S317.

Brechet L, Lucas MF, Doncarli C, Farina D. 2007. Compression of biomedical signals with mother wavelet optimization and best-basis wavelet packet selection. IEEE Trans Biomed Eng. 54(12):2186–2192.

Chudi IP. 2010. Healthcare problems in developing countries. Med Pract Rev. 1(1):9–11.

Correa R, Arini PD, Valentinuzzi ME. 2013. Novel set of vectorcardiographic parameters for the identification of ischemic patients. Med Eng Phys. 35(1):16–22.

Dawson D, Yang H, Malshe M, Bukkapatnam STS, Benjamin B, Komanduri R. 2009. Linear affine transformations between 3-lead (Frank *XYZ* leads) vectorcardiogram and 12-lead electrocardiogram signals. J Electrocardiol. 42:622–630.

Dower GE. 1968. A lead synthesizer for the Frank system to simulate the standard 12-lead electrocardiogram. J Electrocardiol. 1:101.

Dower GE, Yakush A, Nazzal SB, Jutzy RV, Ruiz CE. 1988. Deriving the 12-lead electrocardiogram from four (EASI) electrodes. J Electrocardiol. supplement:182–187.

Edenbrandt L, Pahlm O. 1988. Vectorcardiogram synthesized from a 12- lead ECG: superiority of the inverse Dower matrix. J Electrocardiol. 21(4):361–367.

Feild DQ, Zhou SH, Helfenbein ED, Gregg RE, Lindauer JM. 2008. Technical challenges and future directions in lead reconstruction for reduced-lead systems. J Electrocardiol. 41(6):466–473.

Finlay DD, Nugent CD, Kellett JG, Donnelly MP, McCullagh PJ, Black ND. 2007. Synthesizing the 12-lead electrocardiogram: trends and challenges. Eur J Intern Med. 18(8): 566–570.

Frank E. 1956. An accurate, clinically practical system for spatial vectorcardiography. Circulation. 13:737.

Frank E. 1954. General theory on heart-vector projection. Circ Res. 2:258–270.

Goldberger AL, Amaral LAN, Glass L, Hausdorff JM, Ivanov PCh, Mark RG, Mietus JE, Moody GB, Peng C-K, Stanley HE. 2000. PhysioBank, PhysioToolkit, and PhysioNet: components of a new research resource for complex physiologic signals. Circulation. 101(23):e215–e220.

Gregg RE, Zhou SH, Lindauer JM, Feild DQ, Helfenbein ED. 2008. Where do derived precordial leads fail. J Electrocardiol. 41:546–552.

He B, Wu D. 2001. Imaging and visualization of 3-D cardiac electric activity. IEEE Trans Inf Technol Biomed. 5(3): 181–186.

Hernandez O, Olvera E. 2009. Noise cancellation on ECG and heart rate signals using the undecimated wavelet transform. eTELEMED09. 2009 International Conference on Ehealth, Telemedicine, and Social Medicine; 2009 Feb 1–7; Cancun, Mexico. p. 145–150.

Hoekema R, Uijen GJH, van Oosterum A. 1999. On selecting a body surface mapping procedure. J Electrocardiol. 32 (2):93–101.

Levkov CL. 1987. Orthogonal electrocardiogram derived from the limb and chest electrodes of the conventional 12-lead system. Med Biol Eng Comput. 25:155–164.

Li S, Lin J. 2009. The optimal de-noising algorithm for ECG using stationary wavelet transform. Paper presented at: *WRI World Congress on Computer Science and Information Engineering* 6, p. 469–473.

Liszka KJ, Mackin MA, Lichter MJ, York DW, Pillai D, Rosenbaum DS. 2004. Keeping a beat on the heart. IEEE Pervasive Comput. 3(4):42–49.

Liu SH, Cheng DC, Lin CM. 2013. Arrhythmia Identification with two-lead electrocardiograms using artificial neural networks and support vector machines for a portable ECG monitor system. Sensors. 13:813–828.

Mazomenos EB, Biswas D, Acharyya A, Chen T, Maharatna K, Rosengarten J, Morgan J, Curzen N. 2013. A low-complexity ECG feature extraction algorithm for mobile healthcare applications. IEEE Trans Inf Technol Biomed. 17(2):459–469.

Mazomenos EB, Chen T, Acharyya A, Bhattacharya A, Rosengarten J, Maharatna K. 2012. A time-domain morphology and gradient based algorithm for ECG feature extraction. Paper presented at: 2012 IEEE International Conference on Industrial Technology (ICIT); 2012 Mar 19–21; Athens. p. 117–122.

Nelwan SP, Kors JA, Meij SH. 2000. Minimal lead sets for reconstruction of 12-lead electrocardiograms. J Electrocardiol. supplement:33.

Nelwan SP, Crater SW, Green CL, Johanson P, Dam TB, Meij SH, Simoons ML, Krucoff MW. 2004. Assessment of derived 12-lead electrocardiograms using general and patient-specific reconstruction strategies at rest and during transient myocardial ischemia. Am J Cardiol. 31:1529.

Nelwan SP, Kors JA, Meij SH, Bemmel JH, Simoons ML. 2004. Reconstruction of the 12-lead electrocardiogram from reduced lead sets. J Electrocardiol. 37:11–19.

Peng GC, Bocko MF. 2013. Non-contact ECG sensing employing gradiometer electrodes. IEEE Trans Biomed Eng. 60 (1):179–183.

Prasad S. 2008. Telemedicine takes world class healthcare to rural India. [Online]. Available: http://www.zdnet.com/telemedicine-takes-world-class-healthcareto-rural-india-2062043102/

Riera ARP, Uchida AH, Filho CF, Meneghini A, Ferreira C, Schapacknik E, Dubner S, Moffa P. 2007. Significance of vectorcardiogram in the cardiological diagnosis of the 21st century. Clin Cardiol. 30:319–323.

Rieta JJ, Castells F, Sanchez C, Zarzoso V, Millet J. 2004. Atrial activity extraction for atrial fibrillation analysis using blind source separation. IEEE Trans Biomed Eng. 51 (7):1176–1186.

Scanaill C, Carew S, Barralon P, Noury N, Lyons D, Lyons GM. 2006. A review of approaches to mobility telemonitoring of the elderly in their living environment. Ann Biomed Eng. 34(4):547–563.

Sharma LN, Dandapat S, Mahanta A. 2012. Multichannel ECG data compression based on multiscale principal component analysis. IEEE Trans Inf Technol Biomed. 16(4):730–736.

Vullings R, Peters CHL, Mossavat I, Oei SG, Bergmans JWM. 2010. Bayesian approach to patient-tailored vectorcardiography. IEEE Trans Biomed Eng. 57(3):586–595.

World Health Organisation. 2009. Global health risks: mortality and burden of disease attributable to selected major risks. WHO.

Yang H. 2011. Multiscale recurrence quantification analysis of spatial cardiac vectorcardiogram signals. IEEE Trans Biomed Eng. 58(2):339–347.

Yang H, Bukkapatnam STS, Komanduri R. 2012. Spatiotemporal representation of cardiac vectorcardiogram (VCG) signals. BioMed Eng. 11(16), OnLine.

Yoo J, Yan L, Lee S, Kim H, Yoo HJ. 2009. A wearable ECG acquisition system with compact planar-fashionable circuit board-based shirt. IEEE Trans Inf Technol Biomed. 13 (6):897–902.

Yu B, Xu L, Li Y. 2012. Bluetooth low energy (BLE) based mobile electrocardiogram monitoring system. Paper presented at: 2012 International Conference on Information and Automation (ICIA); 2012 June 6–8; Shenyang. p. 763–767.

Zhang D. 2005. Wavelet approach for ECG baseline wander correction and noise reduction. Paper presented at: IEEE-EMBS 2005. 27th Annual International Conference of the Engineering in Medicine and Biology Society; Sep 01–04; Shanghai. p. 1212–1215.

Appendix

Figures 5 and 6 show the MATLAB code snippet used in this work.

```
[c,t] = wavedec(x,9,'sym10'); %Decomposition of signal
signal = wrcoef('a',c,t,'sym10',9); %Reconstruction of signal from the approx. coefficients
BW_removed_signal = x − signal; %Subtracting the BW from original signal
qmf = MakeONFilter('Symmlet',8);
denoised_signal = recTI(BW_removed_signal,'H',qmf);
```

Figure 5. Snippet of MATLAB code for implementation of preprocessing module.

```
dataset_range = 1000:16000; d_length = 100; d_time = 99; bd = [4:8]; fz = 1300;
% From the dataset considered i.e. first 2^i samples, about 15000 - 20000 samples (dataset_range) were taken from each lead of patients
% from various categories which consisted of about 10-15 PQRST complexes. Out of these complexes the ones mentioned in the variable
% 'bd' i.e. complexes 4 to 8 were taken and averaged. This was done so that there are no conflicts and all the patients in a particular
% category can be operated upon using similar values as arguments. The output from select_train function is a window which includes
% a particular section of the ECG signal and to include/limit exactly one PQRST complex in that window the variables: bd,
% dataset_range, fz, starting point of the window to be considered(d_time) and end point
% of the window (d_length) are regulated and tuned according to the cardiologic disorder (categories). This fine tuning was
% performed upon visual examination of the complete process for all the 12 leads of all the patients category wise. FP= nqrsdetect(Original_signal(dataset_range),1000); %Extraction of fiducial points (FP) from Original signal (OS)
PQRST= select_train(Original_signal(dataset_range),FP,length(FP),1,0,0.5,0,fz); %Extraction of PQRST complexes from OS and FP
len = length(PQRST);
FO = tdmg(mean(PQRST(bd,d_length:len)),1000,1:1:len-d_time);%Feature extraction of Original signal (FO)
clear FP;clear PQRST;
FP= nqrsdetect(Reconstructed_signal(dataset_range),1000);%Extraction of fiducial points (FP) from Reconstructed signal (RS)
PQRST= select_train(Reconstructed_signal(dataset_range),FP,length(FP),1,0,0.5,0,fz);%Extraction of PQRST complexes from RS and FP
len = length(PQRST);
FR = tdmg(mean(PQRST(bd,d_length:len)),1000,1:1:len-d_time);%Feature extraction of Reconstructed signal (FR)
```

Figure 6. Snippet of MATLAB code for implementation of *nqrsdetect·m, select train·m and tdmg·m.*